

Status of QGSJET

Sergey Ostapchenko

University of Karlsruhe, Institut für Experimentelle Kernphysik, 76021 Karlsruhe, Germany

Abstract. Basic physics concepts of the QGSJET model are discussed, starting from the general picture of high energy hadronic interactions and addressing in some detail the treatment of multiple scattering processes, contributions of “soft” and “semihard” parton dynamics, implementation of non-linear interaction effects. The predictions of the new model version (QGSJET II-03) are compared to selected accelerator data. Future developments are outlined and the expected input from the LHC collider for constraining model predictions is discussed.

Keywords: Monte Carlo models, colliders, extensive air showers, cosmic rays

PACS: 12.40.Nn, 13.85.Tp, 96.50.sb, 96.50.sd

INTRODUCTION

Nowadays hadronic Monte Carlo (MC) generators are actively used both in collider and cosmic ray (CR) fields. The idea behind employing such MC models is twofold. First of all, they provide a bridge between rigorous theoretical approaches and corresponding experiments, thus allowing to confront novel ideas against data. On the other hand, MC simulation procedures are an inevitable part of data analysis of modern experiments; an extraction of any new information crucially depends on the understanding of the corresponding detector response, which is mimicked with the help of the MC tools.

Generally, MC models are developed on much less rigorous basis compared to the underlying theoretical approaches and involve a number of additional, sometimes *ad hoc*, assumptions in order to be able to treat complex phenomena studied in experiments. On the other hand, the ultimate goal of model development is to provide an adequate description of the interaction features which are important for this or that particular study, rather than to describe the interaction physics in its full complexity.

In the CR field, high energy MC generators are mainly used for the description of the development of so-called extensive air showers (EAS) – nuclear-electro-magnetic cascades induced by primary cosmic ray (PCR) particles (to present knowledge, protons or nuclei) in the atmosphere. Studying various EAS characteristics, primarily the position of the shower maximum X_{\max} (the depth in g/cm^2 , where maximal number of charged particles is observed) and the numbers of e^\pm (N_e) and of muons (N_μ) at ground, one infers information on the PCR energy spectrum and their composition. These techniques set a number of requirements on the corresponding MC generators. First of all, one is obliged to treat very general (minimum bias) hadronic collisions in the cascade. Furthermore, of special importance are model predictions for the inelastic hadron-nucleus interaction cross section, which makes a direct impact on the X_{\max} . Going further, calculated EAS characteristics appear to be very dependent on the model predictions for forward particle spectra, first of all, on the relative energy difference between the initial hadron and

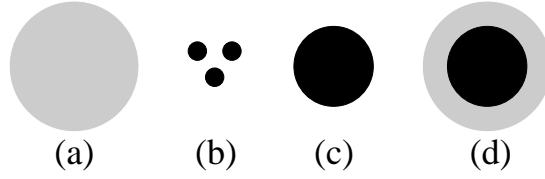


FIGURE 1. Proton profile as viewed in soft (a), hard (b), semihard (c), and general (d) interactions.

the most energetic secondary one – the so-called inelasticity K_{inel} . But the most crucial requirement to CR interaction models is the predictive power, as one has to extrapolate the available theoretical and experimental knowledge from the energies of present day colliders up to the highest CR energies, which are as high as 10^{20} eV!

However, the problem under study offers also a number of simplifications. For example, one is not sensitive to “fine” details of hadronic final states, e.g., to production of short-lived resonances, whose effect is smoothed out during the cascade development, or to the contribution of high p_t hadrons, which are typically collinear with the initial particle direction ($p_t/E \ll 1$) and thus do not influence the lateral shape of the shower. The same applies to the production of charm, bottom, or more exotic (e.g., SUSY) particles, for which one obtains rather small inclusive cross sections (compared to pions and kaons) to influence charged particle content of EAS, and which are produced mainly at central rapidities, thus having a negligible influence on K_{inel} , hence, on X_{max} . To resume, CR interaction models are generators of very “typical” (mb level) interactions.

HIGH ENERGY INTERACTIONS: QUALITATIVE PICTURE

The general picture for high energy hadronic collision is the one of a multiple scattering process, being mediated by parton (quark and gluon) cascades proceeding between the two hadrons. An inelastic interaction involves a number of elementary hadron production contributions, where the coherence of the underlying parton cascades is broken and partons fragment into secondary hadrons. In addition, it may contain multiple elastic re-scatterings, where the coherence is preserved and all the partons from the corresponding chains recombine back to their parent hadrons, without a production of secondaries. In turn, elastic scattering is obtained when only elastic sub-processes occur.

With the energy increasing, the number of elementary re-scattering processes grows rapidly, due to the larger phase space for parton emissions. In addition, one expects a qualitative change in the structure of the underlying parton cascades. At comparatively low energies, all the partons are characterized by small transverse momenta; high p_t emissions are suppressed by the smallness of the corresponding running coupling, $\alpha_s(p_t^2)$. By the uncertainty principle, each emission is characterized by a large displacement of the produced parton in the transverse plane, $\Delta b^2 \sim 1/p_t^2$. Thus, with the energy increasing further, such “soft” parton cascades rapidly expand towards larger impact parameters, while the density of partons per unit transverse area remains small, the hadron looking “grey”, as depicted in Fig. 1 (a). However, at sufficiently high energies an important contribution comes from so-called “semi-hard” and “hard” parton cascades, in which some or all partons have comparatively high transverse momenta [1]. There, the

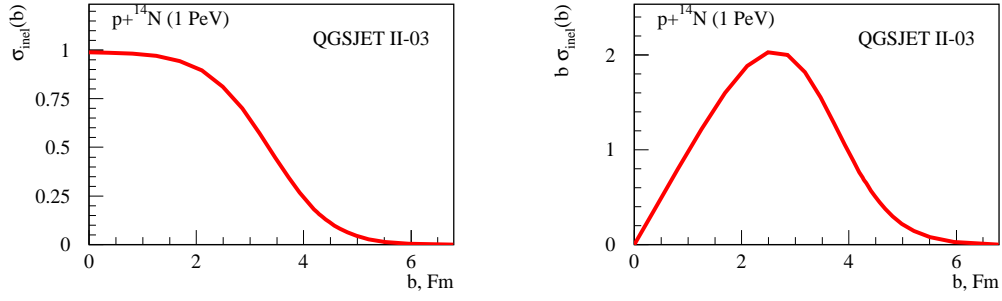


FIGURE 2. Interaction profile (left) and relative contributions of various impact parameters to the inelastic cross section (right) for proton-nitrogen collision at 10^6 GeV.

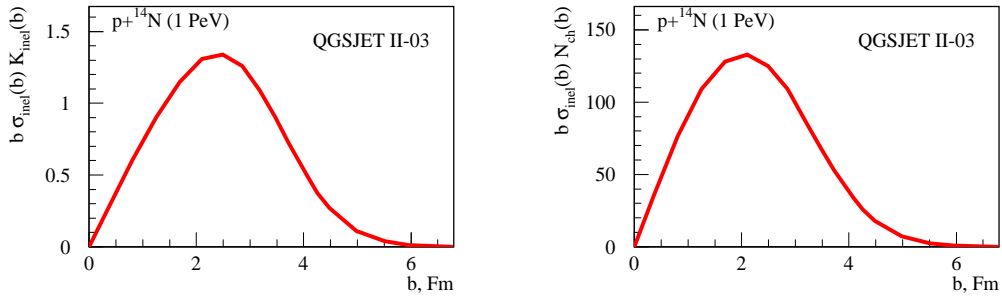


FIGURE 3. Contributions of various impact parameters to K_{pN}^{inel} (left) and to N_{pN}^{ch} (right) at 10^6 GeV.

smallness of the strong coupling $\alpha_s(p_t^2)$ is compensated by a high parton density and by large logarithmic ratios of the longitudinal and transverse momenta for successive parton emissions. Purely hard cascades, which start, e.g., from valence quarks and contain only high p_t partons, do not expand transversely, $\Delta b^2 \sim 1/p_t^2$ being small, and lead to an increase of parton density in small areas in the transverse plane – see Fig. 1 (b), while giving a negligible contribution to the total cross section. Contrary to that, typical semi-hard re-scatterings are two-step processes: first, parton branchings proceed with a small momentum transfer and the cascade develops towards larger impact parameters; next, high p_t parton emissions become effective, leading to a rapid rise of the parton density at a given point in the transverse plane. As a result, the region of high parton density extends to large impact parameters (Fig. 1 (c)) and the contribution dominates in the very high energy limit. General hadronic interactions include all the mentioned mechanisms; hadrons in high energy collisions look as shown in Fig. 1 (d): there is an extended “black” region of high density, dominated by the semihard processes, and around it there is a “grey” region of low density, formed by purely soft parton cascading. In the “black” region one expects strong non-linear parton effects to emerge, which result in the saturation of parton densities and in the suppression of soft parton emissions [1]. On the other hand, such effects are weak in the “dilute” peripheral region.

What is the relative importance of the two regimes? As shown in Fig. 2 (left), in 1 PeV proton-nitrogen collisions the “black” region (with the interaction probability $\sigma_{\text{inel}}(b) \simeq 1$) extends to impact parameters $b \sim 2$ Fm. On the other hand, Fig. 2 (right) shows that most of the inelastic collisions actually happen at $b > 2$ Fm, i.e. they are mostly

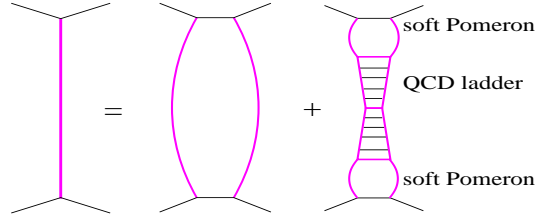


FIGURE 4. A “general Pomeron” is the sum of the “soft” and the “semihard” ones – correspondingly the 1st and the 2nd graphs in the r.h.s.

peripheral ones. Similar conclusions follow if we investigate relative contributions of central and peripheral interactions to the inelasticity K_{pN}^{inel} and the multiplicity of charged particles N_{pN}^{ch} of the interaction, as shown in Fig. 3: K_{pN}^{inel} is dominated by peripheral collisions, while for N_{pN}^{ch} central and peripheral contributions are of equal importance.

QGSJET MODEL

General model strategy to describe high energy hadronic (nuclear) interactions consists of the following steps: i) to describe an “elementary” interaction (parton cascade), i.e. to define the corresponding scattering amplitude and the procedure to convert partons into final hadrons; ii) to treat multiple scattering processes in the framework of the Gribov’s Reggeon approach [2]; iii) to describe particle production as a superposition of a number of “elementary” interactions. It is worth stressing that the advantages of the pQCD formalism can be used here only partially and only at the first of the above-described steps, as most of the elementary parton cascades develop partly (or even entirely) in the nonperturbative “soft” region of small parton virtualities $|q^2| \simeq p_t^2$.

In the particular case of the QGSJET model [3], one introduces a cutoff Q_0^2 between the “soft” and “hard” parton dynamics, applies DGLAP [4] formalism for $|q^2| \geq Q_0^2$, and employs a phenomenological “soft” Pomeron description for the nonperturbative ($|q^2| < Q_0^2$) parton cascades. This way, an elementary interaction between hadrons a and d is described by a “general Pomeron” eikonal $\chi_{ad}^{\text{P}}(s, b)$ (imaginary part of the corresponding amplitude), which consists of two terms: the soft Pomeron eikonal $\chi_{ad}^{\text{Psoft}}(s, b)$, representing a pure nonperturbative (all $|q^2| < Q_0^2$) parton cascade, and the so-called “semihard Pomeron” eikonal $\chi_{ad}^{\text{Psh}}(s, b)$: $\chi_{ad}^{\text{P}}(s, b) = \chi_{ad}^{\text{Psoft}}(s, b) + \chi_{ad}^{\text{Psh}}(s, b)$. The latter corresponds to a piece of QCD parton ladder sandwiched between two soft Pomerons and represents a cascade which at least partly develops in the region of high $|q^2|$, as shown in Fig. 4 [3] (see also [5]).

To obtain cross sections for various final states, one makes use of the optical theorem, which relates the total sum of contributions of all final states to the imaginary part of the elastic amplitude for hadron-hadron scattering, hence, to the contributions of various unitarity cuts of elastic scattering diagrams. The so-called Abramovskii-Gribov-Kancheli (AGK) cutting rules [6] state that only certain classes of cut diagrams are important in the high energy limit and allow to relate such contributions to particular final states of interest. For example, the non-diffractive cross section can be expressed

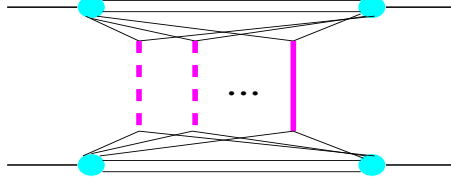


FIGURE 5. Typical inelastic interaction contains a number of elementary particle production processes, described by cut Pomerons (broken thick lines), and any number of elastic re-scatterings – uncut Pomeron exchanges (unbroken thick lines).

as a sum of contributions corresponding to a given number n of elementary production processes (“cut” Pomerons) and to any number of elastic re-scatterings (see Fig. 5):

$$\sigma_{ad}^{\text{ND}}(s) = \sum_{n=1}^{\infty} \sigma_{ad}^{(n)}(s) = \sum_{n=1}^{\infty} \left\{ \sum_{j,k} C_a^{(j)} C_d^{(k)} \int d^2b \frac{[2\lambda_a^{(j)} \lambda_d^{(k)} \chi_{ad}^{\text{P}}(s,b)]^n}{n!} e^{-2\lambda_a^{(j)} \lambda_d^{(k)} \chi_{ad}^{\text{P}}(s,b)} \right\},$$

where $C_a^{(j)}$ and $\lambda_a^{(j)}$ are correspondingly relative weights and relative strengths of diffraction eigenstates for hadron a [7]. In turn, elastic and diffractive cross sections are obtained when elastic scattering diagrams are cut between Pomerons, with no one being cut, selecting elastic or diffractive intermediate hadron states in the cut plane.

Finally, particle production is treated as a break out and a hadronization of strings of the color field; in soft processes such strings are stretched between constituent partons of the initial hadrons, to which the Pomerons are coupled. In case of semihard processes, one treats explicitly, within the DGLAP formalism, the production of partons (gluons and (anti-)quarks) of high transverse momenta ($p_t^2 > Q_0^2$); the strings are then formed between both these “hard” partons and the “soft” constituent ones.

Importantly, the generalization from hadron-hadron to hadron-nucleus and nucleus-nucleus interactions proceeds in a parameter-free way, both for cross section calculations and for particle production treatment [8].

NONLINEAR EFFECTS (QGSJET II)

Extending model description to very high energies, one has to treat non-linear interaction effects, which come into play when individual parton cascades start to overlap in the corresponding phase space and to influence each other. Such effects are expected to be extremely important at very high energies and small impact parameters, i.e. in the “black” region of high parton densities, where they lead to the parton density saturation [1] and to significant reduction of secondary particle production. On the other hand, non-linear parton dynamics starts to manifest itself already at comparatively low energies and large impact parameters, the experimental indication being the rapid energy rise of the high mass diffraction cross section in the ISR energy range [9].

Treating independent parton cascades effectively as Pomeron exchanges, the corresponding non-linear effects are described in the Reggeon Field Theory (RFT) as Pomeron-Pomeron interactions [10]. A resummation of the corresponding (so-called

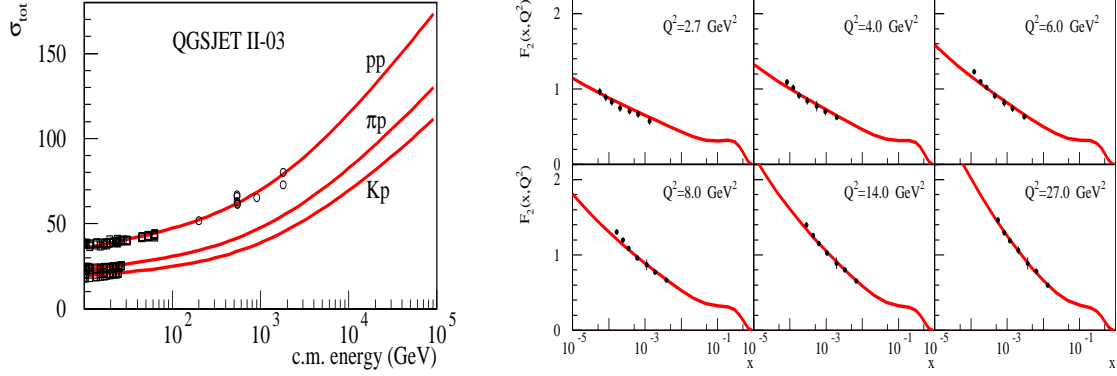


FIGURE 6. Calculated total hadron-proton cross sections (left) and proton SF F_2 (right) compared to experimental data (points) [13, 14].

enhanced) RFT diagrams has been worked out recently [11], both for elastic scattering contributions and for the corresponding unitarity cuts, and implemented in the QGSJET-II model [12]. The basic assumption of the approach was that Pomeron-Pomeron coupling proceeds via parton processes at comparatively low virtualities $|q^2| < Q_0^2$ and can be described using phenomenological multi-Pomeron vertices of eikonal type. The approach allowed one to obtain a reasonable consistency with experimental data on the total proton-proton cross section and on the proton structure function (SF) F_2 (see Fig. 6), using a fixed energy-independent cutoff $Q_0^2 = 2.5 \text{ GeV}^2$, i.e. neglecting possible parton saturation effects at higher virtuality ($|q^2| > Q_0^2$) scales.

It is worth stressing that in the discussed approach, like in the usual linear scheme described in the preceeding Section, cross section calculations and particle production treatment are performed within the same framework. While the former are expressed via hadron-hadron elastic scattering amplitude, which is obtained by the resummation of the underlying *uncut* RFT diagrams, the latter is based on the computation of *unitarity cuts* of the very same diagrams, such that summary contributions of cuts of certain topologies define relative weights of particular final states. The corresponding results have been obtained in [11] in the form of recursive equations, which allowed one to develop a MC algorithm to generate various configurations of interactions, including diffractive ones, in an iterative fashion.

It is noteworthy that the obtained consistency between hadronic cross sections and SFs, demonstrated in Fig. 6, is highly nontrivial. By construction, the discussed scheme preserves the QCD factorization for inclusive jet spectra, which allows one to describe correctly high p_t hadron production. However, the usual correspondence between the semihard eikonal $\chi_{ad}^{\text{Psh}}(s, b)$ and the inclusive cross section $\sigma_{ad}^{\text{jet}}(s, Q_0^2)$ for the production of hadron jets of $p_t > Q_0$, namely $\int d^2b \chi_{ad}^{\text{Psh}}(s, b) \equiv \sigma_{ad}^{\text{jet}}(s, Q_0^2)$, which held in the original QGSJET model and which is still the cornerstone of all other MC generators, is no longer valid in the nonlinear scheme. This is because there are two types of enhanced RFT diagrams which contribute to χ_{ad}^{Psh} . The diagrams of the first kind provide factorizable corrections which can be absorbed in the parton distribution functions (PDFs) and which do not violate the above relation. On the other hand, the diagrams

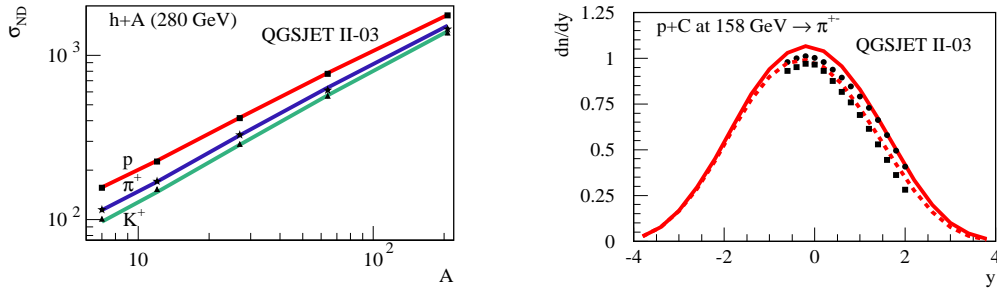


FIGURE 7. Left: calculated A -dependence of non-diffractive hadron-nucleus cross sections at 280 GeV compared to experimental data (points) [15]. Right: calculated rapidity distributions of π^\pm in pp interactions at 158 GeV compared to the data of the NA49 Collaboration [16].

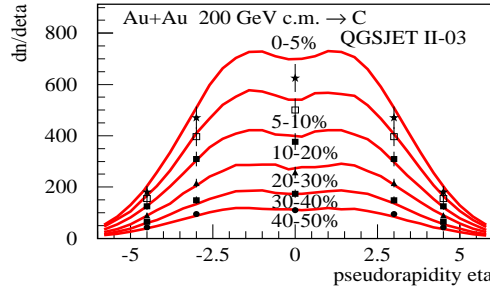


FIGURE 8. Pseudorapidity distributions of charged secondary particles in Au-Au collisions of different “centralities”; QGSJET-II results (lines) are compared to BRAHMS data [17].

of the second kind are nonfactorizable ones and can not be accounted for by any modification of the PDFs. As discussed in more detail in [11, 12], such contributions precisely cancel each other in the inclusive jet spectra, the latter being expressed in the usual way via universal PDFs of free hadrons (which contain, however, nonlinear corrections of the first kind). However, there is no such cancellation in the interaction eikonal and correspondingly in the partial cross sections for particular *exclusive* final states. The latter are expressed via nonuniversal (process-dependent) PDFs, which are “probed” during interaction and are thus affected by the surrounding medium [12].

Finally, the generalization from hadron-hadron to hadron-nucleus (nucleus-nucleus) interactions is again performed in a parameter-free way. In the latter case, one obtains automatically an A -enhancement of the screening effects, due to the coupling between Pomerons connected to different nucleons. At fixed target energies, one obtains an impressive agreement with measured non-diffractive hadron-nucleus cross sections (Fig. 7 (left)); the predicted pion spectra also match the data reasonably well (Fig. 7 (right)).

Concerning RHIC data on central heavy ion collisions, those generally can not be used to judge on the goodness of a MC model for CR applications – because the physics of very dense parton systems is of secondary importance for EAS development. However, such comparisons help to understand the range of applicability of a particular model approach. In the QGSJET II case, one may expect that the model overestimates secondary particle multiplicity in such reactions – as additional screening corrections, connected to Pomeron-Pomeron coupling in the region of high parton virtualities ($|q^2| >$

Q_0^2), are not taken into consideration. The obtained reasonably good agreement with the data (Fig. 8) indicates that such effects are yet small at the RHIC energies.

OUTLOOK

The principal novelty of the QGSJET II model is a microscopic treatment of nonlinear interaction effects in hadronic and nuclear collisions. In this aspect, it provides a reference point for all other hadronic MC generators, where such corrections are introduced at a much more phenomenological level, typically by means of empiric energy-dependent parameterizations of some model parameters (see, e.g. [18]). Generally, QGSJET-II stays in a reasonable agreement with present accelerator data, including ones of the RHIC collider. Moreover, the model predictions at much higher energies seem to match experimental EAS data as well [19].

Further model improvement is presently in progress to account for the contributions of so-called Pomeron “loop” diagrams. Being suppressed in the present scheme at small impact parameters [11], they may provide finite corrections to elastic scattering amplitude at large b , thus influencing model calibration on the basis of observed $\sigma_{pp}^{\text{tot}}(s)$.

From the experimental side, all present MC models will substantially benefit from future measurements of total and diffractive proton-proton cross sections at the LHC by the CMS and FP420 experiments, the two quantities largely determining the high energy extrapolation of model predictions. On the other hand, the forthcoming studies of forward neutron and photon production by the LHCf experiment will allow to constrain model treatment of the hadronization process.

REFERENCES

1. L. V. Gribov, E. M. Levin and M. G. Ryskin, *Phys. Rep.* **100**, 1 (1983).
2. V. N. Gribov, *Sov. Phys. JETP* **26**, 414 (1968).
3. N. N. Kalmykov, S. S. Ostapchenko and A. I. Pavlov, *Bull. Russ. Acad. Sci. Phys.* **58**, 1966 (1994); *Nucl. Phys. B (Proc. Suppl.)* **52B**, 17 (1997).
4. V. N. Gribov and L. N. Lipatov, *Sov. J. Nucl. Phys.* **20**, 438 (1972); L. N. Lipatov, *Sov. J. Nucl. Phys.* **20**, 94 (1975);
5. H. J. Drescher et al., *J. Phys. G* **25**, L91 (1999); S. Ostapchenko et al., *J. Phys. G* **28**, 2597 (2002).
6. V. A. Abramovskii, V. N. Gribov and O. V. Kancheli, *Sov. J. Nucl. Phys.* **18**, 308 (1974). G. Altarelli and G. Parisi, *Nucl. Phys. B* **126**, 298 (1977).
7. A. B. Kaidalov, *Phys. Rep.* **50**, 157 (1979).
8. N. N. Kalmykov and S. S. Ostapchenko, *Phys. Atom. Nucl.* **56**, 346 (1993).
9. K. Goulianos, *Phys. Lett. B* **358**, 379 (1995).
10. O. V. Kancheli, *JETP Lett.* **18**, 274 (1973); J. L. Cardi, *Nucl. Phys. B* **75**, 413 (1974).
11. S. Ostapchenko, *Phys. Lett. B* **636**, 40 (2006); hep-ph/0612068.
12. S. Ostapchenko, *Phys. Rev. D* **74**, 014026 (2006); *Nucl. Phys. B (Proc. Suppl.)* **151**, 143 (2006).
13. C. Caso et al., *Eur. Phys. J. C* **3**, 1 (1998).
14. S. Chekanov et al. (ZEUS Collab.), *Nucl. Phys. B* **713**, 3 (2005).
15. A. S. Carroll et al., *Phys. Lett. B* **80**, 319 (1979).
16. C. Alt et al. (NA49 Collab.), *Eur. Phys. J. C* **45**, 343 (2006).
17. I. G. Bearden et al. (BRAHMS Collab.), *Phys. Rev. Lett.* **88**, 202301 (2002).
18. F. W. Bopp et al., *Phys. Rev. D* **49**, 3236 (1994); J. Dischler and T. Sjostrand, *Eur. Phys. J. direct C* **3**, 2 (2001); S.-Y. Li and X.-N. Wang, *Phys. Lett. B* **527**, 85 (2002).
19. A. Haungs et al. (KASCADE Collab.), these proceedings.